GSA Data Repository 2019391

Meyer, G.G., Brantut, N., Mitchell, T.M., andMeredith, P.G., 2019, Fault reactivation and strain partitioning across the brittle-ductile transition: Geology, v. 47, https://doi.org/10.1130/G46516.1

SUPPLEMENTAL INFORMATION DR1

The material chosen for our experiments was Carrara marble, selected because it undergoes a brittle to fully plastic transition at room temperature and at moderate confining pressure (≈ 300 MPa, Paterson, 1958; Rutter, 1974; Fredrich et al., 1989). Cylindrical samples of 100 mm in length (L) and 40 mm in diameter were cored, and their faces ground parallel. Two pairs of strain gauges were bonded to the middle of each core in order to record matrix strain (see supplementary Figure S2). The samples were jacketed in a Viton sleeve equipped with piezoelectric transducers arranged to measure horizontal (diametral) P wave speed (e.g., Brantut et al., 2014). The jacketed samples were placed in an oil-medium triaxial apparatus. The applied load was measured with an external load cell, and total axial shortening ΔL was recorded externally by a pair of linear variable differential transformers (LVDT), corrected for the deformation of the loading train (Figure 1, inset). The confining pressure (P_c) is imposed with an electromechanical pump, and is controlled with a precision of 0.4 MPa.

Experiments were conducted in two stages. During the first stage, samples were pre-faulted by loading at P_c = 5 MPa until localized brittle failure occurred. Following failure, an additional increment of shortening $\Delta L/L$ of either 0.1% or 1% was allowed to accumulate before proceeding to the second stage, in order to test any effect of accumulated fault slip on the transition. In the second stage, the confining pressure was increased stepwise from 5 to 80

MPa in 5 or 10 MPa increments. At each pressure step, the pre-faulted samples were re-loaded at an axial shortening rate of $\dot{\varepsilon}=10^{-5}$ s^{-1} until 0.1% of irrecoverable axial shortening was accumulated, and then unloaded before proceeding to the next pressure step.

An additional experiment was performed in order to investigate the effect of shortening rate. Two rates were used at each confining pressure step: first, the sample was loaded at $\dot{\varepsilon}=10^{-4}$ s^{-1} until 0.1% shortening was accumulated; second, the sample was partially unloaded (by approximately 20 MPa) and then reloaded at the lower rate of $\dot{\varepsilon}=10^{-6}$ s^{-1} until a further 0.1% shortening.

Throughout each experiment, horizontal P wave speeds (perpendicular to the compression axis) were measured repeatedly using the same method as described by Brantut et al. (2014).

The external LVDTs record the total axial shortening, which is the sum of the strain in the rock matrix ε_{matrix} and the projected slip on the fault $\delta \cos(\theta)/L$, such that $\Delta L/L = \varepsilon_{matrix} + \delta \cos(\theta)/L$, where δ denotes the fault slip and θ is the fault angle with respect to the compression axis. By contrast, the strain gauges record only the matrix strain off the main fault (over an area of about 1 cm^2). The contribution of slip to the total shortening can therefore be determined from taking the difference between the strain gauge and LVDT readings.

REFERENCES CITED

Brantut, N., Heap, M. J., Baud, P., and Meredith, P. G., 2014, Mechanisms of time-dependent deformation in porous limestone: Journal of Geophysical Research: Solid Earth, v. 119, p. 5444–5463.

Fredrich, J. T., Evans, B., and Wong, T.-F., 1989, Micromechanics of the brittle to plastic transition in Carrara marble: Journal of Geophysical Research: Solid Earth, v. 94, p. 4129–4145.

Paterson, M. S.,1958, Experimental Deformation and Faulting in Wombeyan Marble: GSA Bulletin, v. 69, p. 465–476.

Rutter, E. H., 1974, The influence of temperature, strain rate and interstitial water in the experimental deformation of calcite rocks: Tectonophysics, v. 22, p. 311–334.

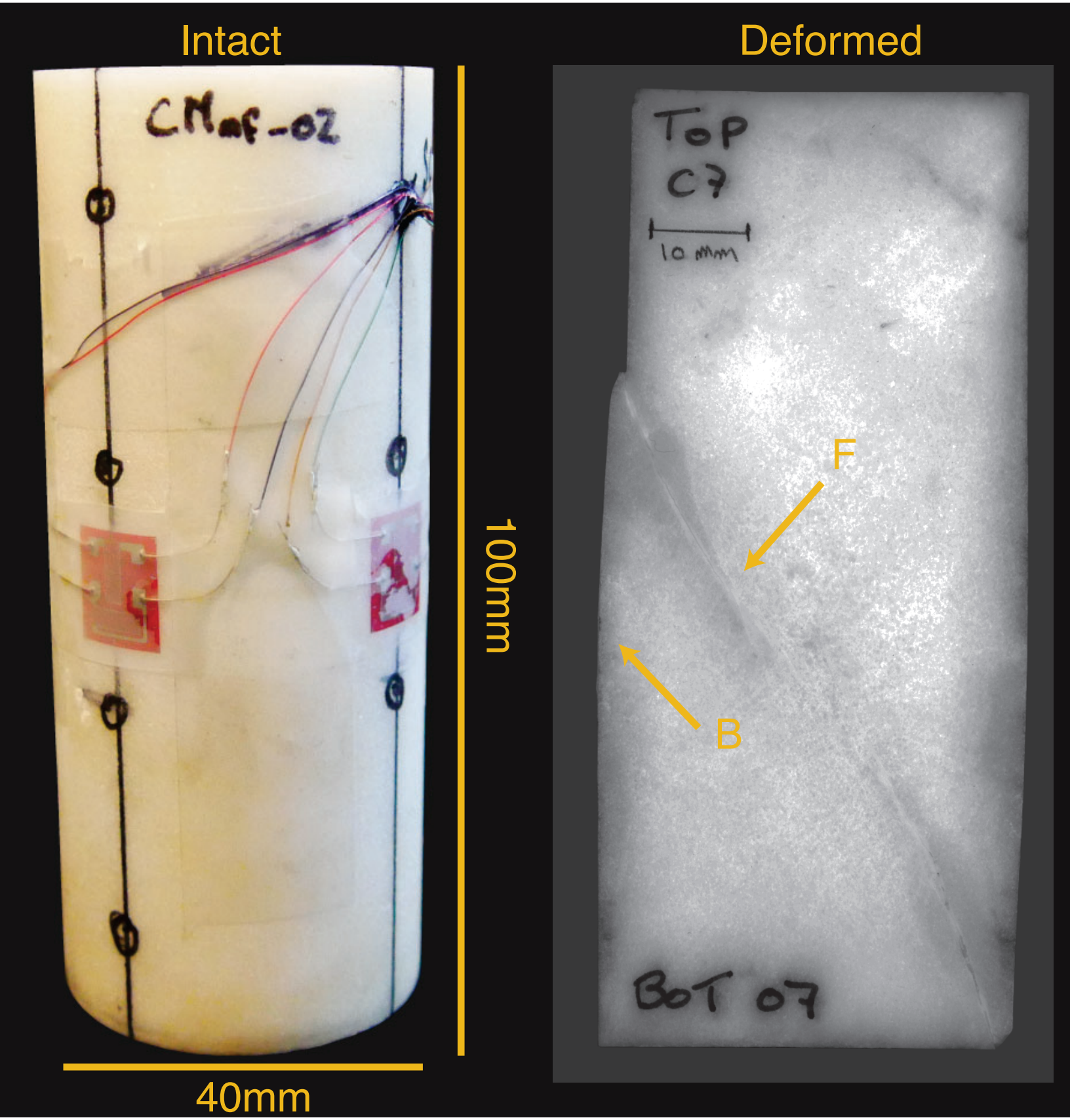

Figure DR1: Left: picture of a sample equipped with strain gauges and prior to jacketing. Right: scan of the cross cut section of a deformed sample. The picture has been altered to improve contrast. F represents the sample-scale fault and B the ductile barrelling.

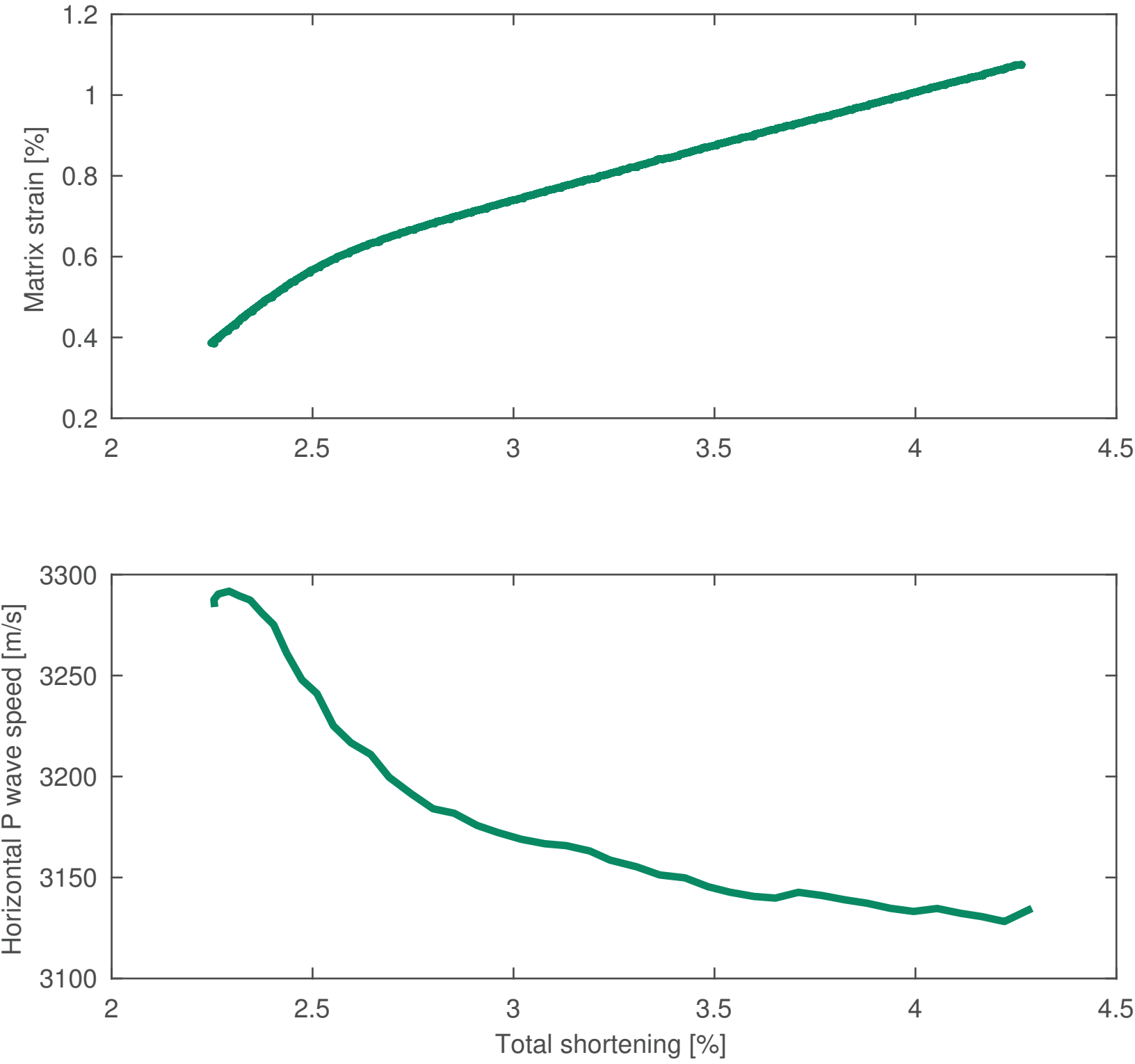

Figure DR2: Mechanical and horizontal P wave data for a single-cycle experiment at P_c=35 MPa. The sample was placed in conditions such as the strain partitioning between slip and matrix strain would be roughly 50/50.

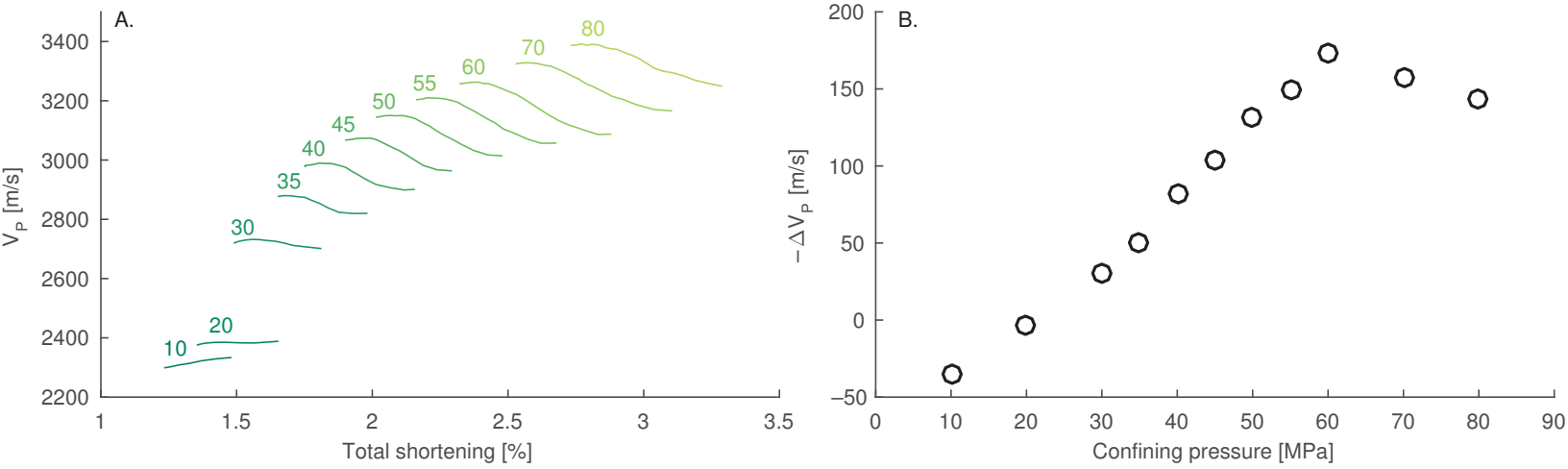

Figure DR3: Left: the evolution of horizontal P-wave for a travel path across the fault. The numbers indicate the confining pressure. Right: P wave velocity drop during each cycle for a given travel path.

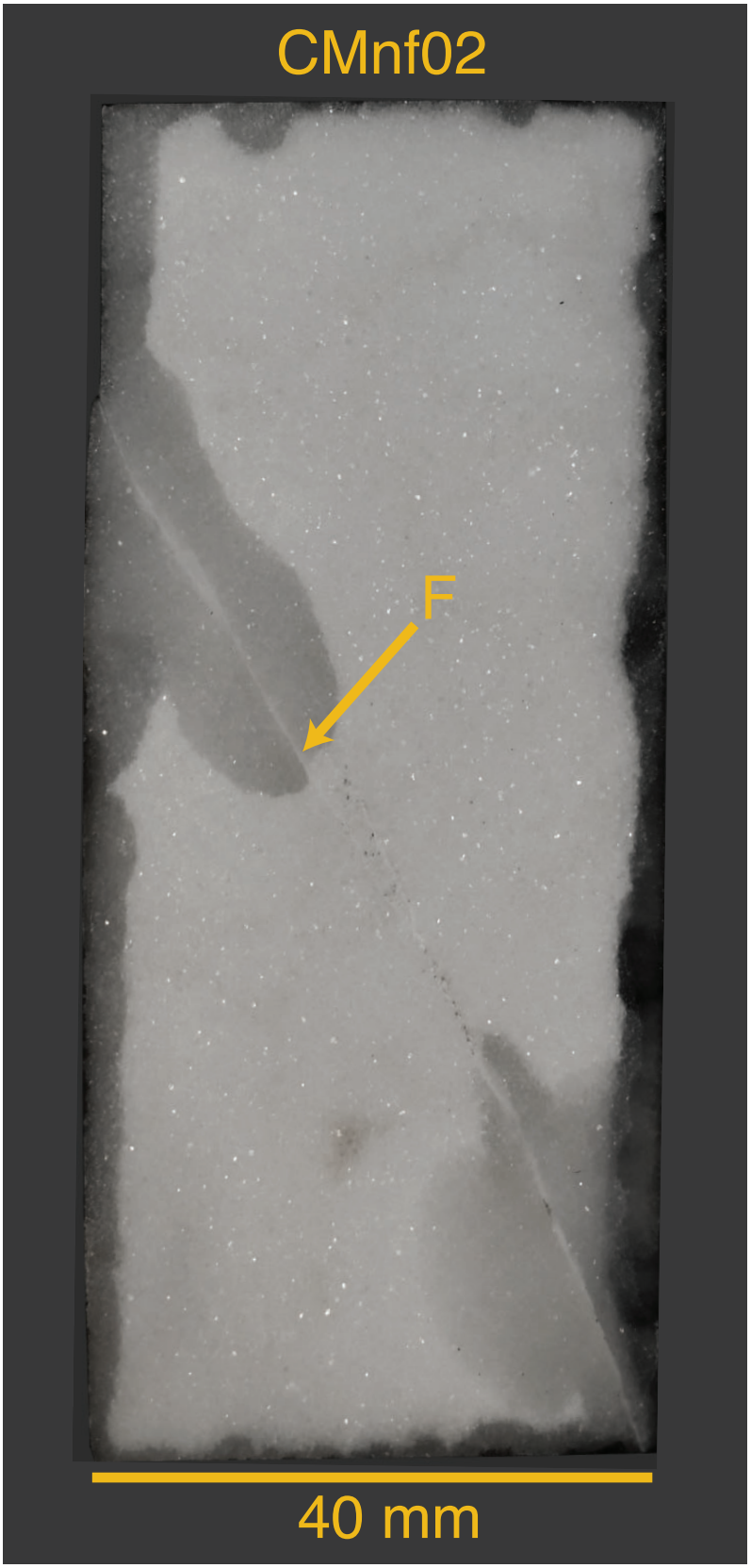

Figure DR4: Post mortem picture of CMnf02, a sample that has undergone the full localised-ductile transition. The picture has been altered to improve contrast. The dark coloration is due to epoxy resin impregnation. F represents the sample-scale fault.

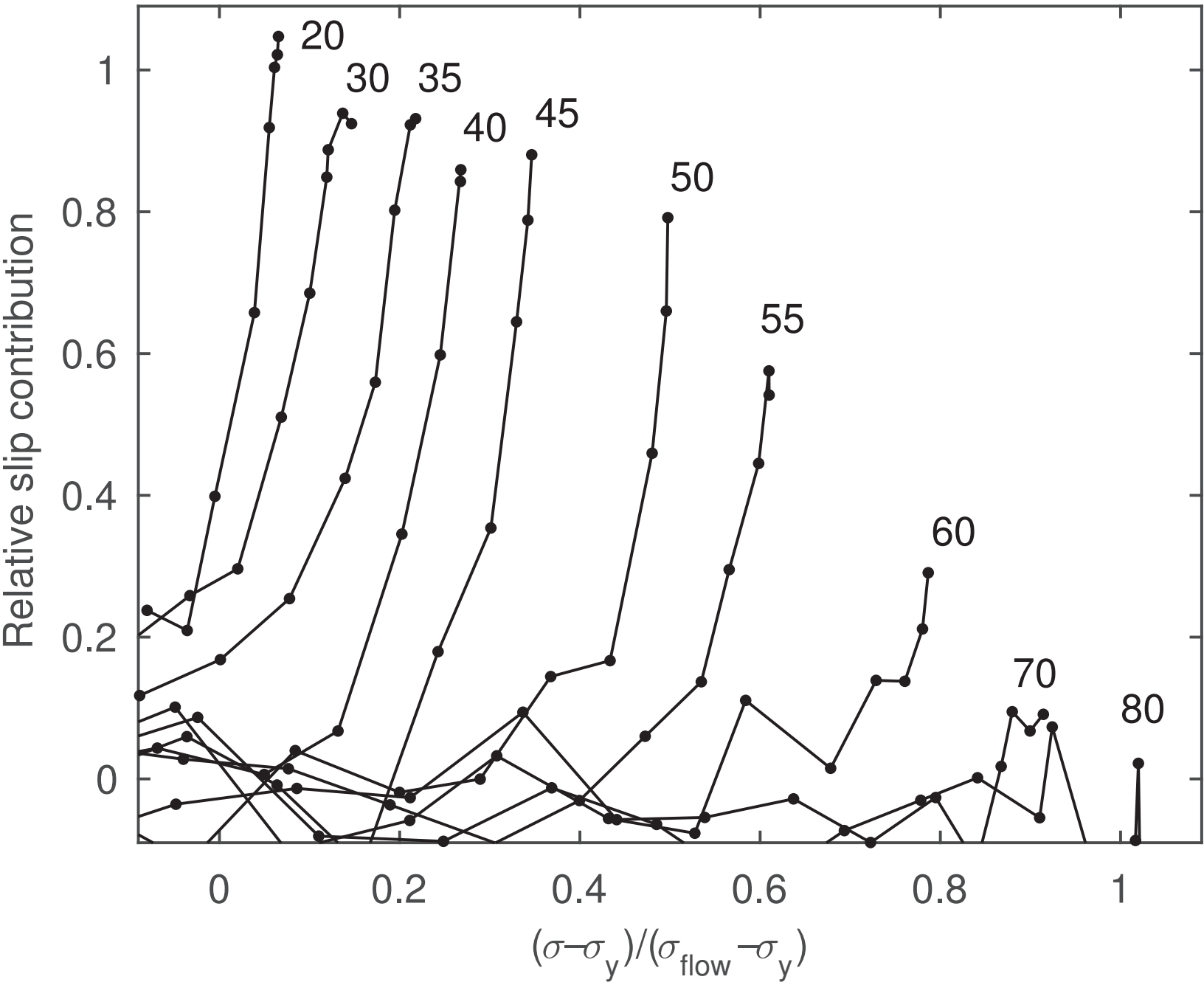

Figure DR5: Relative slip contribution against $(\sigma_f-\sigma_y)/(\sigma_{flow}-\sigma_y)$. Numbers represent the confining pressure during each cycle.

Table DR1. Summary of the experimental conditions.

Sample	P_c [MPa]	Accumulated $\Delta L/L$ [%]	Shortening rate [s^{-1}]
CMnf02	10-80	0.1	10^{-5}
CMnf05	35	0.1	10^{-5}
CMnf08	20-50	1	10^{-5}
CMnf09	10-60	0.1	10^{-4} & 10^{-6}